Biologically inspired coupled antenna beampattern design

2010 Bioinspir. Biomim. 5 046003

(http://iopscience.iop.org/1748-3190/5/4/046003)

Bioinsp. Biomim. **5** (2010) 046003 (11pp) doi:10.1088/1748-3182/5/4/046003

Biologically inspired coupled antenna beampattern design

Murat Akçakaya and Arye Nehorai

Department of Electrical and Systems Engineering, Washington University in St Louis, St Louis, MO 63130, USA

E-mail: makcak2@ese.wustl.edu and nehorai@ese.wustl.edu

Received 16 April 2010
Accepted for publication 19 October 2010
Published 10 November 2010
Online at stacks.iop.org/BB/5/046003

Abstract

We propose to design a small-size transmission-coupled antenna array, and corresponding radiation pattern, having high performance inspired by the female *Ormia ochracea*'s coupled ears. For reproduction purposes, the female *Ormia* is able to locate male crickets' call accurately despite the small distance between its ears compared with the incoming wavelength. This phenomenon has been explained by the mechanical coupling between the *Ormia*'s ears, which has been modeled by a pair of differential equations. In this paper, we first solve these differential equations governing the *Ormia ochracea*'s ear response, and convert the response to the pre-specified radio frequencies. We then apply the converted response of the biological coupling in the array factor of a uniform linear array composed of finite-length dipole antennas, and also include the undesired electromagnetic coupling due to the proximity of the elements. Moreover, we propose an algorithm to optimally choose the biologically inspired coupling for maximum array performance. In our numerical examples, we compute the radiation intensity of the designed system for binomial and uniform ordinary end-fire arrays, and demonstrate the improvement in the half-power beamwidth, sidelobe suppression and directivity of the radiation pattern due to the biologically inspired coupling.

(Some figures in this article are in colour only in the electronic version)

1. Introduction

Localization of sources and targets with high accuracy is important in many civil and military applications, attracting significant attention over the past few decades [1–6]. These applications require antenna arrays with high radiation performance. Most existing array design methods rely on the inter-elemental time delay of the antenna array to control radiation pattern (beampattern) characteristics [7]. The performance of the antenna array is directly proportional to the size of the array's electrical aperture, such that large aperture arrays are required to achieve highly directed, narrow beampatterns with low sidelobe levels (SLLs). However, for tactical and mobile applications, many civil and military sensing systems are confined to small spaces, requiring small-sized arrays, which hampers their radiation performance.

In this paper, we propose a beampattern design approach to achieve high performance with small aperture arrays. The approach is inspired by a parasitoid tachinid fly called *Ormia ochracea*. To perpetuate its species, a female *Ormia* must find a male field cricket using the cricket's mating call. The female *Ormia* has a remarkable ability to locate these crickets very accurately using binaural (two-ear) cues (interaural differences in intensity and arrival time from an incident acoustic wave). This is unexpected due to the significant mismatch between the wavelength of the cricket's call (about 7 cm) and the distance between the fly's ears (about 1.2 mm) which gives rise to cues that are extremely small to be detectable by the central nervous system of the fly [8–13].

Experimental research in [14] explains that the *Ormia*'s localization ability arises from a mechanical coupling between its ears, modeled as a system consisting of spring and dash-pots (with six key parameters: $\{(c_i, k_i) : i = 1, 2, 3\}$) as shown in figure 1. In the equivalent mechanical system, the intertympanal bridge (the cuticular connecting structure) is assumed to consist of two rigid bars connected at the pivot through a coupling spring k_3 and dash-pot c_3. The

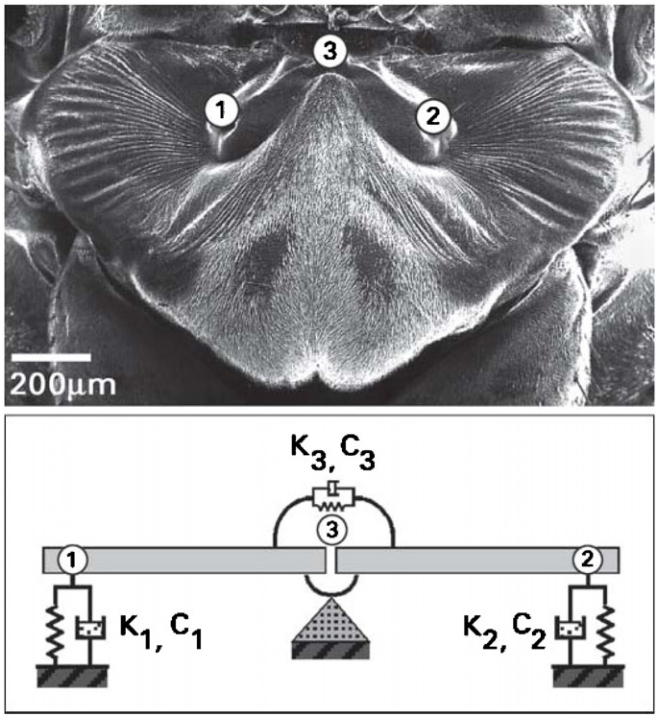

Figure 1. Mechanical model of the female *Ormia ochracea*'s ears. Reproduced with permission from [14]. Copyright 1995, Acoustic Society of America.

springs and dash-pots located at the extreme ends of the bridge approximate the dynamical properties of the tympanal membranes, sensory organs and surrounding structures in the *Ormia*'s two ears.

In our previous work [15], we analyzed the localization accuracy of the *Ormia*'s coupled ears using a statistical approach, namely by computing the Cramér–Rao bound (CRB)[1] [16]. We showed quantitatively that the coupling improves the accuracy of direction of arrival (DOA) estimation in the presence of interference and noise.

The concept of electrically small antenna arrays with high radiation performance, superdirective (supergain) arrays, is quite old [7] and has attracted antenna researchers for the last few decades. Different methods have been proposed to achieve the superdirectivity, namely by decoupling the antennas (reducing the effects of the undesired electromagnetic coupling among the antennas) and changing the current distributions applied to the array elements [17–20]. In this paper, inspired by the female *Ormia*'s coupled ears, we show that applying biologically inspired coupling (BIC) among antennas is beneficial to achieve high radiation performance. Our goal is to demonstrate the effect of the BIC on the radiation performance. The implementation of the BIC system and the investigation of the relationship between the superdirective arrays and the BIC system are left as a future work. We would like to note that our approach, namely employing BIC, might also be used to complement the existing superdirective array design methods that overcome issues, for example, like the effect of the undesired coupling on individual antenna impedance.

[1] The Cramér–Rao bound is a universal minimum bound on the mean-square error value that can be achieved by any unbiased estimation algorithm.

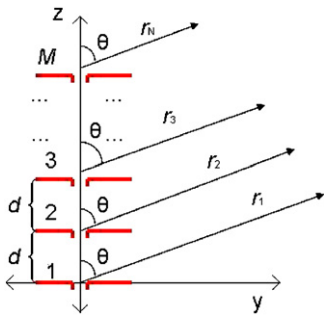

Figure 2. Far-field radiation geometry of M-element antenna array.

The rest of the paper is organized as follows. In section 2, we introduce the array-factor design for a uniform linear array (ULA) inspired by the *Ormia*. First, we solve the second-order differential equations governing the *Ormia*'s coupled ear response. Then we convert this response to fit the desired radio frequencies. Together with the undesired electromagnetic coupling among the array elements (due to their proximity), we include the BIC in the array factor. In section 3, we assume finite-length dipoles as the antenna elements and compute the radiation intensity, and accordingly the directivity gain, half-power beamwidth (HPBW) and side lobe level (SLL) as radiation performance measures. In section 4, we introduce our algorithm for the optimum coupling selection. In section 5, we compare the radiation performances of the biologically inspired coupled and standard antenna arrays, demonstrating the improvement due to the BIC. By standard antenna array we refer to a system without BIC. Finally we provide concluding remarks in section 6.

2. Array factor

In this section, we compute the array factor of the proposed biologically inspired ULA. We start with the array factor of a standard ULA, positioned without loss of generality along the z-axis (see figure 2). Since we focus on systems confined in small spaces, we also consider the undesired electromagnetic coupling between the array elements.

Under the far-field radiation and narrow-band signal assumption, we modify the ULA factor to include the undesired coupling between the elements (see also [21]):

$$\mathrm{AF}(\theta) = \sum_{m=1}^{M} p_m \exp(-j(m-1)(\omega\Delta + \beta)), \qquad (1)$$

where

- $\mathrm{AF}(\theta)$ is the radiation pattern (desired amplitude and phase in each direction) of M-element array assuming isotropic antennas, which depends on the positions and excitations of the sensing elements in the system;
- $\boldsymbol{p} = [p_1, \ldots, p_M]^T = \boldsymbol{C}\boldsymbol{v}_g$ is the vector of the currents on the antennas;

- $\boldsymbol{v}_g = [v_1, \ldots, v_M]^T$ is the vector of the generator (excitation) voltages at the input of the antennas;
- $\boldsymbol{C}$ is the undesired electromagnetic coupling between the array elements, (a transformation matrix, transforming generator voltages to the induced currents on each antenna);
- $\omega = 2\pi f$ with f as the frequency of the radiated signal;
- $\Delta = \frac{d \sin\theta}{v}$ is the inter-element time difference;
- d is the inter-element distance;
- v is the speed of signal propagation in the medium;
- θ is the elevation angle (see figure 2) and
- β is the excitation phase.

We compute $\boldsymbol{C}$ similar to [21] as a function of self and mutual impedances between the antennas (see also discussions in [22] and [23]). We summarize the computation of $\boldsymbol{C}$ in the appendix. When the mutual impedances are zero, when there is no electromagnetic coupling, $\boldsymbol{C}$ reduces to a diagonal matrix. We compute the self and mutual impedances, assuming finite-length dipole antennas as the elements of the array, as explained in [7, chapter 8]; see also section 5. Note that the standard literature often ignores $\boldsymbol{C}$, which is reasonable for sufficiently large inter-elemental distances.

The usual goal of the array-factor design is to select the excitation voltages, $\boldsymbol{v}_g$, and phase, β, to obtain a desired radiation pattern. Our goal is to include the BIC in the array factor for fixed $\boldsymbol{v}_g$ and β values and demonstrate the improvement in the directivity gain, HPBW and SLL of the radiation pattern.

Next we generalize (1) to include also the coupling biologically inspired by the *Ormia*'s coupled ears. First we obtain the response of the *Ormia*'s coupled ears. We then convert this response to fit the desired radio frequencies, and modify the array factor to also include BIC. Moreover, at the end of this section, we provide a physical explanation of the BIC used in the array design.

In our work on biologically inspired antenna array and DOA estimation [24], we demonstrated our approach to obtain the frequency response of the *Ormia*'s ears and how to shift it to the desired radio frequencies. For the sake of completeness and clarity of the presentation of the current work, we include these parts in sections 2.1 and 2.2.

2.1. Response of the Ormia's coupled ears

To obtain the response of the *Ormia*'s coupled ears, we solve the second-order differential equations governing the mechanical model proposed in [14] for the *Ormia*'s ears (figure 1), and find the corresponding transfer function. Note that these equations represent a two-input two-output filter system (see also section 2.4). The governing differential equations are

$$\begin{bmatrix} k_1+k_3 & k_3 \\ k_3 & k_2+k_3 \end{bmatrix}\begin{bmatrix} y_1 \\ y_2 \end{bmatrix} + \begin{bmatrix} c_1+c_3 & c_3 \\ c_3 & c_2+c_3 \end{bmatrix}\begin{bmatrix} \dot{y}_1 \\ \dot{y}_2 \end{bmatrix} + \begin{bmatrix} m_0 & \\ & m_0 \end{bmatrix}\begin{bmatrix} \ddot{y}_1 \\ \ddot{y}_2 \end{bmatrix} = \begin{bmatrix} x_1(t,\Delta) \\ x_2(t,\Delta) \end{bmatrix}, \quad (2)$$

where

- $x_i(t, \Delta)$, $i = 1, 2$, are the input signals;
- $y_i(t)$, $i = 1, 2$, are the displacements of each ear and
- m_0, k's and c's are the effective mass, spring and dash-pot constants, respectively.

To solve the differential equations and obtain the transfer function (and hence the frequency response) of the system, we apply the Laplace transform[2] to (2) assuming zero initial values:

$$\begin{bmatrix} Y_1(s) \\ Y_2(s) \end{bmatrix} = 1/P(s)\begin{bmatrix} D_2(s) & -N(s) \\ -N(s) & D_1(s) \end{bmatrix}\begin{bmatrix} X_1(s) \\ X_2(s) \end{bmatrix}, \quad (3)$$

where

- $Y_1(s)$ and $Y_2(s)$ are the Laplace transforms of $y_1(t)$ and $y_2(t)$,
- $X_1(s)$ and $X_2(s)$ are the Laplace transforms of $x_1(t)$ and $x_2(t)$,
- $D_1(s) = m_0 s^2 + (c_1 + c_3)s + k_1 + k_3$ and $D_2(s) = m_0 s^2 + (c_2 + c_3)s + k_2 + k_3$,
- $N(s) = c_3 s + k_3$ (coupling effect),
- $P(s) = D_1(s)D_2(s) - N^2(s)$ is the characteristic function.

We obtain the Laplace transform of the impulse responses associated with (2) by substituting

$$x_1(t) = \delta(t) \rightarrow X_1(s) = 1,$$
$$x_2(t) = x_1(t - \Delta) \rightarrow X_2(s) = \mathrm{e}^{-s\Delta}.$$

Then the system responses are

$$H_1(s, \Delta) = (D_2(s) - N(s)\mathrm{e}^{-s\Delta})/P(s),$$
$$H_2(s, \Delta) = (D_1(s)\mathrm{e}^{-s\Delta} - N(s))/P(s). \quad (4)$$

For $s = j\omega$, we obtain the frequency responses of the *Ormia*'s coupled ears. See figures 3 and 4 for the amplitude and phase responses of the *Ormia*'s ears. To demonstrate the effect of the mechanical coupling, we compare the coupled response of the *Ormia*'s ear with a response assuming zero coupling ($N(s) = 0$). We observe that the coupling amplifies the amplitude and phase differences between the responses of the *Ormia*'s two ears. The figures are obtained using the effective mass, spring and dash-pot constants experimentally obtained in [14].

2.2. Converting to desired radio frequencies for the array response design

We now modify the frequency response of the *Ormia*'s ears to fit the desired radio frequencies. We achieve this conversion by re-computing the poles of the transfer function in (3), the roots of $P(s) = D_1(s)D_2(s) - N^2(s) = 0$, for the frequencies of interest. We shift the resonance frequencies of the system by changing the imaginary parts of the poles. This corresponds to changing the system parameters, namely mass, spring and dash-pot constants defined in the analogous mechanical model (see (2)). Note that we do not necessarily need to change these parameters using the same scaling constant. We can scale the resonant frequency locations (controlling the imaginary parts of the poles) and the real parts of the poles using different

[2] See our approach in [15] for the state-space solution of the *Ormia*'s ear responses. In this work, we focus on the Laplace transform solution which simplifies the procedure.

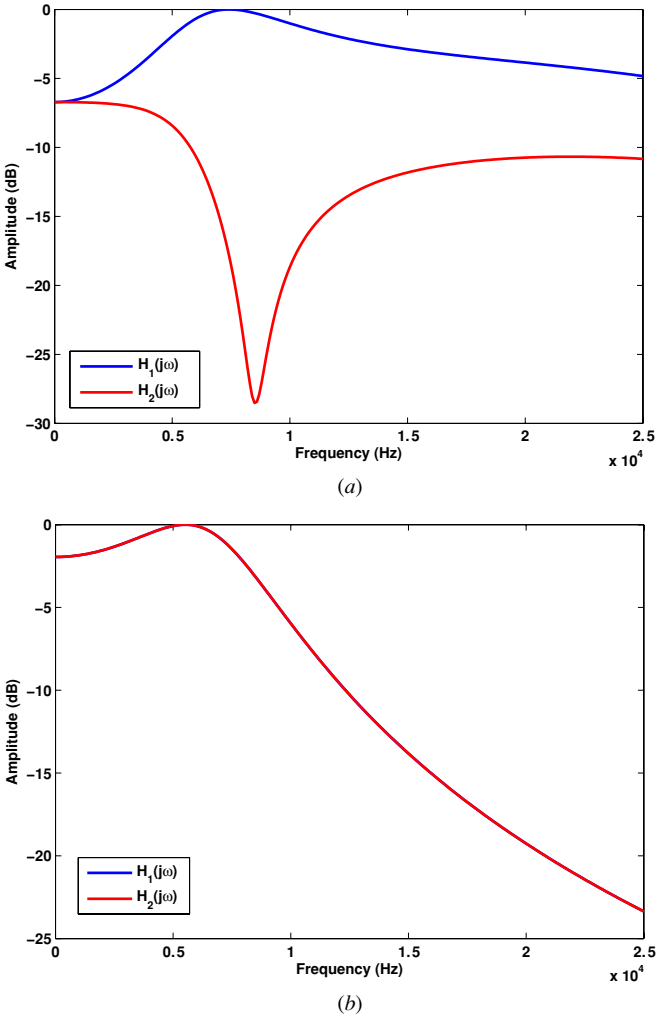

Figure 3. Amplitude responses of the *Ormia ochracea*'s two ears. (a) Coupled system. (b) Uncoupled system.

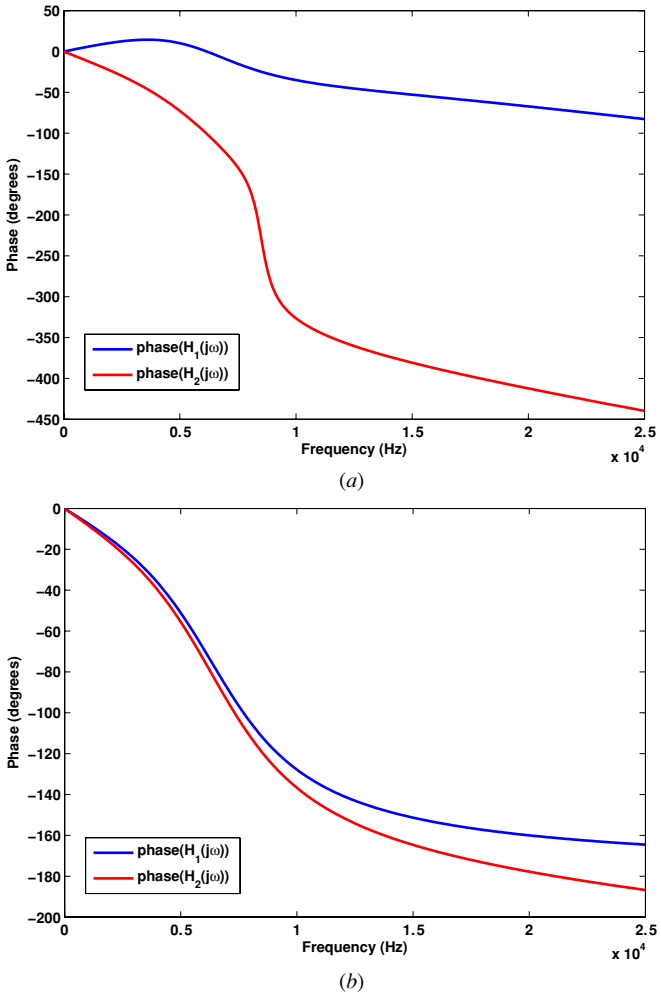

Figure 4. Phase responses of the *Ormia ochracea*'s two ears. (a) Coupled system. (b) Uncoupled system.

constants. We will keep the real parts as free variables which will enable us to optimize the coupling without modifying the resonant frequencies; see section 4. Our purpose is to preserve a coupling structure similar to figures 3 and 4 which amplifies the differences between the amplitude and phase responses of the system outputs. See for example figure 5 for the amplitude and phase responses of the converted system with $f = 1$ GHz as the desired frequency.

We obtain the ratio between the frequency responses

$$\frac{H_2(\omega, \Delta)}{H_1(\omega, \Delta)} = \frac{D_1(j\omega)\mathrm{e}^{-j\omega\Delta} - N(j\omega)}{D_2(j\omega) - N(j\omega)\mathrm{e}^{-j\omega\Delta}}. \tag{5}$$

choosing the frequency ω depending on the application (see also section 5).

2.3. Biologically inspired coupled array factor

To apply the BIC concept to the array factor in (1), we replace the exponential terms in (1) with the ratio in (5):

$$\mathrm{AF_I}(\theta) = \sum_{m=1}^{M} p_m \left(\frac{H_2(\omega, \Delta, \beta)}{H_1(\omega, \Delta, \beta)} \right)^{(m-1)}, \tag{6}$$

where

$$\frac{H_2(\omega, \Delta, \beta)}{H_1(\omega, \Delta, \beta)} = \frac{D(j\omega)\exp(-j(\omega\Delta + \beta)) - N(j\omega)}{D(j\omega) - N(j\omega)\exp(-j(\omega\Delta + \beta))}, \tag{7}$$

with $D(j\omega)$ and $N(j\omega)$ as defined after (3), substituting $s = j\omega$. We assume identical antennas $D_1(j\omega) = D_2(j\omega) = D(j\omega)$. The ratio in (5) generalizes the exponential terms in (1) to include the BIC.

Note that $N(j\omega)$ represents the BIC, and when there is no coupling ($N(j\omega) = 0$), $\mathrm{AF_I}(\theta)$ in (6) reduces to $\mathrm{AF}(\theta)$ in (1). In this paper, we analytically demonstrate the biologically inspired beampattern design. The actual implementation is left for a future work.

2.4. Filter interpretation

In this section, we explain the physical effects of the BIC on the linear antenna array.

- In the receiving mode, the mechanical coupling is represented as a two-input two-output filter (figure 6), amplifying the differences between the outputs of the system; see figures 3 and 4.

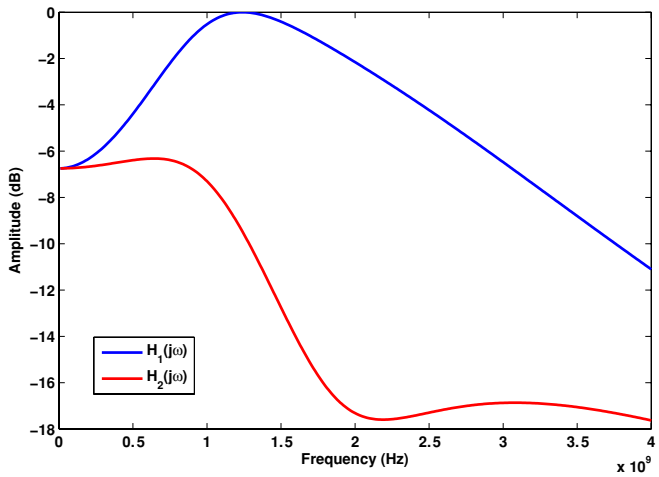

(*a*)

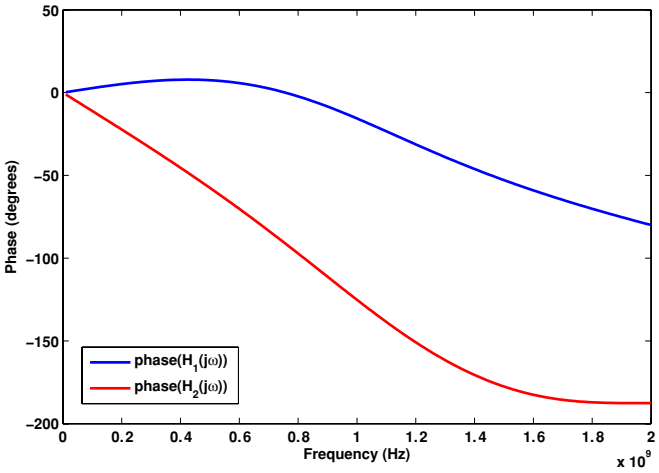

(*b*)

Figure 5. (a) Amplitude and (b) phase responses of the converted system.

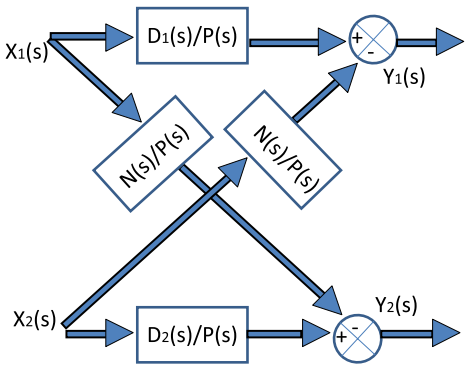

Figure 6. The *Ormia*'s coupled ears as a two-input two-output filter system.

- Since the mechanical coupling amplifies the amplitude and phase differences between the frequency responses of the *Ormia*'s ears [15], it effectively creates larger distance between successive antennas, a virtual array with a larger aperture.
- To apply the biological coupling concept in the transmitting mode, we include the BIC in the array factor (in addition to the undesired electromagnetic coupling). Thus, we generate a virtual array with a larger aperture. Larger aperture improves the radiation performance of the transmitting system (providing higher directivity gain, lower HPBW and SLL).
- For higher order antenna arrays, the structure in (6) corresponds to applying the BIC between successive antennas, such that each antenna is coupled to its immediate neighboring antennas. Therefore, for every two successive antennas, the BIC creates a virtual array with a larger aperture, and hence a larger aperture for the entire array.

3. Radiation intensity, directivity, HPBW and SLL

In this section, we describe our measures to analyze the radiation performance. First, taking into account the antenna factor (element factor) and the BIC, we compute the radiation intensity of the antenna array in a given direction [7]:

$$U_{\mathrm{I}}(\theta,\phi) = [\mathrm{EF}(\theta,\phi)]_{\mathrm{n}}^2 [\mathrm{AF}_{\mathrm{I}}(\theta)]_{\mathrm{n}}^2, \tag{8}$$

where

- $[\mathrm{EF}(\theta,\phi)]_{\mathrm{n}}$ is the normalized element factor, far-zone electric field of a single element (in our work we assume that the array is formed with finite-length dipoles; see also section 5);
- $[\mathrm{AF}_{\mathrm{I}}(\theta)]_{\mathrm{n}}$ is the normalized array factor;
- $U_{\mathrm{I}}(\theta,\phi)$, the radiation intensity in a given direction, is the power radiated from an antenna array per unit solid angle.
- Hence, the radiated power P_{rad} is

$$P_{\mathrm{rad}} = \int_0^{2\pi}\int_0^{\pi} U_{\mathrm{I}}(\theta,\phi)\sin\theta \,\mathrm{d}\theta\,\mathrm{d}\phi, \tag{9}$$

where θ and ϕ are the elevation and azimuth angles, respectively, and $\sin\theta\,\mathrm{d}\theta\,\mathrm{d}\phi$ is the unit solid angle.

Using the radiation intensity, we consider the following measures to analyze the performance of the beampattern design.

- The directivity, $D_{\mathrm{I}}(\theta,\phi)$, is the ratio of the radiation intensity in a given direction to the average radiation intensity:

$$D_{\mathrm{I}}(\theta,\phi) = \frac{4\pi U_{\mathrm{I}}(\theta,\phi)}{P_{\mathrm{rad}}}, \tag{10}$$

where $\frac{1}{4\pi}P_{\mathrm{rad}}$ is the average radiation intensity over all angles. In our work, for comparison purposes, we consider the directivity gain in a desired direction (at elevation $\theta = 0^\circ$ and azimuth $\phi = 90^\circ$; see also section 5).
- The HPBW, in terms of the elevation angle, θ, for a fixed azimuth angle, ϕ. The HPBW is defined as the angle between two half-power directions [7].
- The SLL defined as the maximum value of the radiation pattern in any direction other than the desired one (direction other than $\theta = 0^\circ$ on $\phi = 90^\circ$ plane for our case).

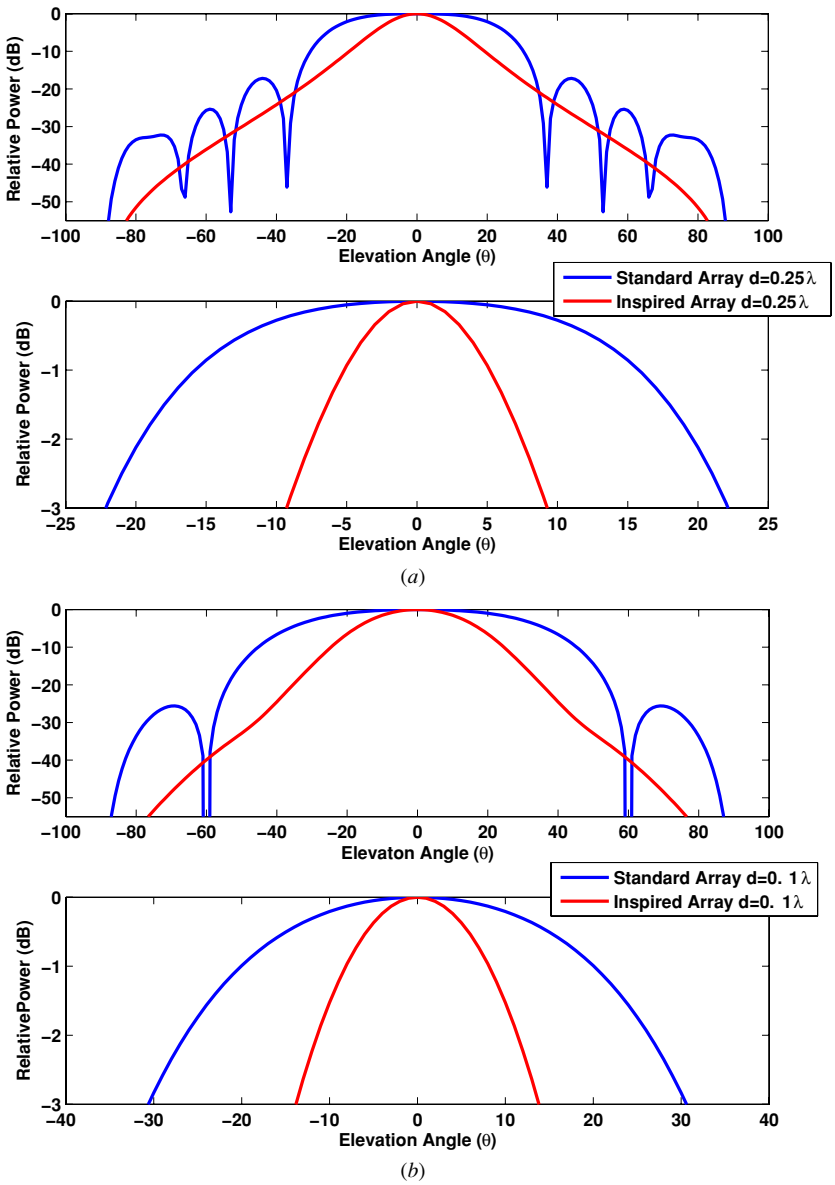

Figure 7. Power pattern of the uniform standard and inspired ordinary end-fire antenna arrays for (a) $d = 0.25\lambda$, (b) $d = 0.1\lambda$ inter-element spacings. Bottom halves of the figures (a) and (b) present the HPBW.

The directivity gain, HPBW and SLL measure how effectively the power is directed (steered) in a given direction. For a good performance, it is desirable to have large $D_1(\theta, \phi)$, small SLL and narrow HPBW in a desired direction.

4. Optimization of the biologically inspired coupling

In this section, we develop a method to maximize the radiation performance by optimizing the BIC. We first introduce the optimization parameters, and then formulate a cost function for optimum radiation pattern design.

Recall from section 2.2 that we change the imaginary parts of the poles of the characteristic function to shift the resonance frequencies of the system response while keeping the real parts as free variables. Therefore, under the constraints that we explain below, we have the freedom to choose the real parts for optimum coupling design. We compute the poles of the system as a function of its parameters (ks, cs and m_0). Recalling the discussions after (3), we assume identical antennas ($D_1(s) = D_2(s) = D(s)$, and hence $k_1 = k_2 = k$, $c_1 = c_2 = c$), and write the characteristic function as

$$\begin{aligned} P(s) &= D(s)^2 - N(s)^2 \\ &= m_0^2((s^2 + b_1 s + a_1)^2 - (b_2 s + a_2)^2), \end{aligned} \tag{11}$$

where $a_1 = (k + k_3)/m_0$, $a_2 = k_3/m_0$, $b_1 = (c + c_3)/m_0$ and $b_2 = c_3/m_0$. We assume that the parameters a_1, a_2, b_1 and b_2 are positive. Then we obtain the roots (the poles of the system) as

$$p_{1,2} = -r_1 \pm \sqrt{i_1} \tag{12}$$

$$p_{3,4} = -r_2 \pm \sqrt{i_2}, \tag{13}$$

where $r_1 = \frac{1}{2}(b_1 + b_2)$, $r_2 = \frac{1}{2}(b_1 - b_2)$, $i_1 = \frac{1}{4}((b_1 + b_2)^2 - 4(a_1 + a_2))$ and $i_2 = \frac{1}{4}((b_1 - b_2)^2 - 4(a_1 - a_2))$. In order to

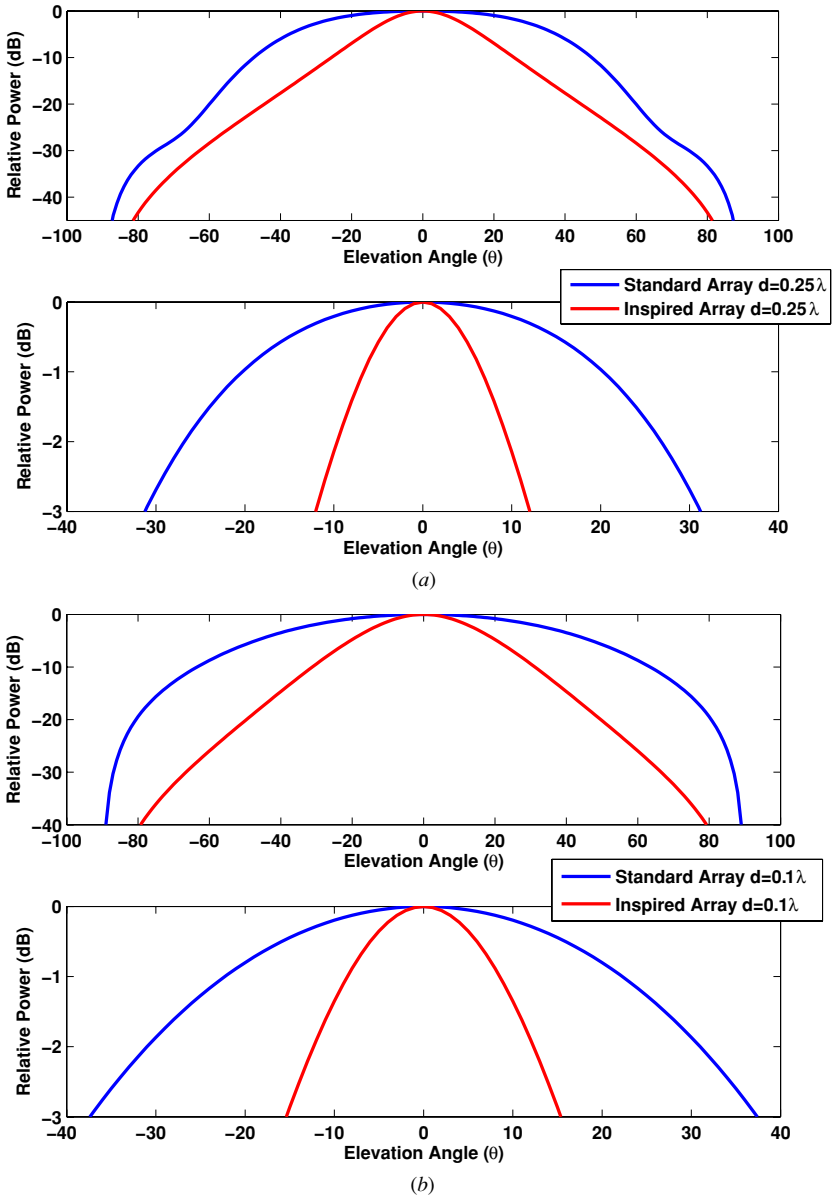

Figure 8. Power pattern of the binomial standard and inspired end-fire antenna arrays for (a) $d = 0.25\lambda$, (b) $d = 0.1\lambda$ inter-element spacings. Bottom halves of the figures (a) and (b) present the HPBW.

change the resonance frequencies, we change the values of the imaginary parts such that $i_1 = -(2\pi f_1)^2$ and $i_2 = -(2\pi f_2)^2$, where f_1 and f_2 are the resonant frequencies. We set r_1 and r_2 as the free parameters. We have the freedom to control the real parts as long as $r_1 > r_2$ due to the positivity assumption on the parameters a_1, a_2, b_1 and b_2.

Next we formulate the optimization problem to improve the radiation performance. For an antenna array, we choose the directivity gain in a desired direction as the utility function to be maximized. This is a reasonable choice since the directivity gain is also related to the SLL and the HPBW of the radiation pattern. Generally it is true that the patterns with smaller SLL and HPBW values have larger directivity gain. Therefore, we formulate the problem as

$$\begin{array}{ll} \text{maximize} & D_1(\theta, \phi) \\ \text{subject to} & r_1 - r_2 > 0, \end{array} \tag{14}$$

where θ and ϕ are the elevation and azimuth of the desired direction of transmission.

5. Numerical examples

In this section, we compare the radiation performances of the biologically inspired coupled and standard antenna arrays. We plot the radiation pattern and compare the directivity gain, HPBWs and sidelobe attenuation of these systems using the following scenario. Moreover, we demonstrate our results on optimum BIC selection. In the following discussions, by inspired array we refer to an antenna array with BIC.

- We consider uniform (uniform excitation voltages) ordinary and binomial (binomial expansion coefficients as the excitation voltage values) end-fire arrays [7, chapter 8], maximum at $\theta = 0^\circ$; then $\beta = -w\Delta$.

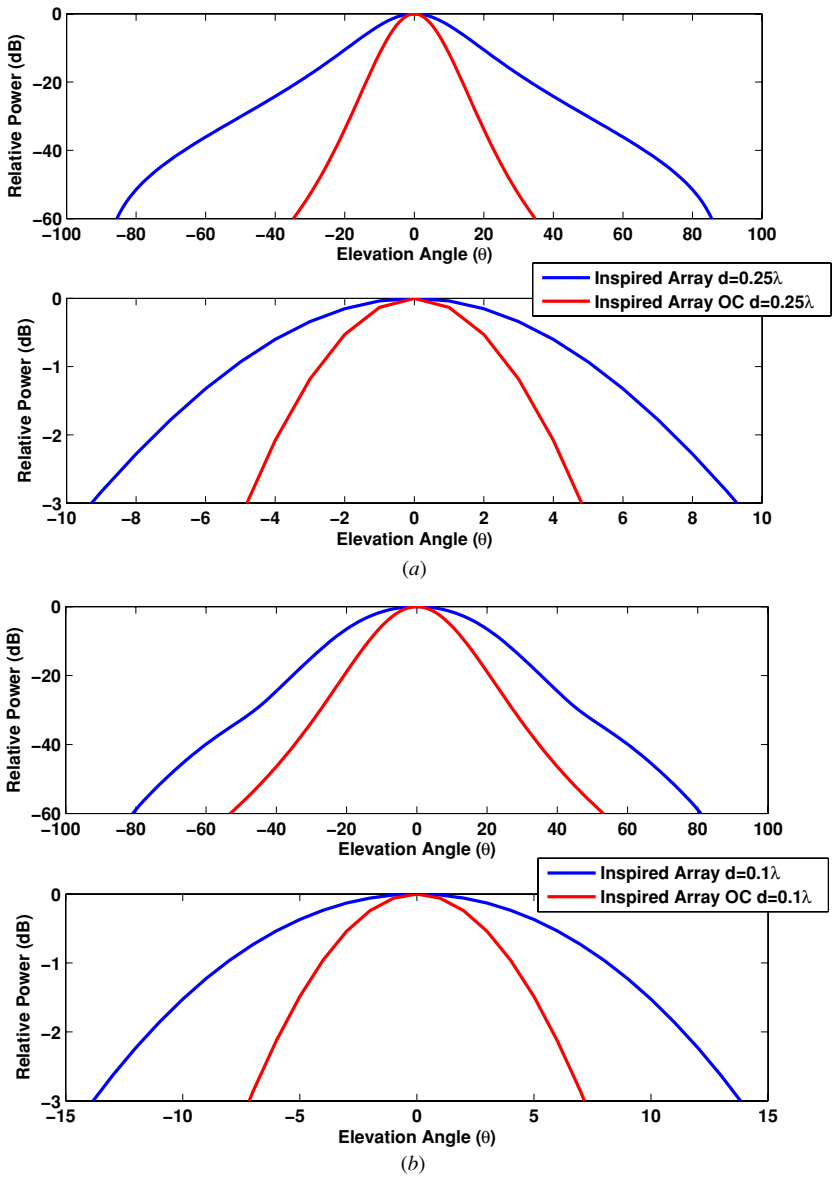

Figure 9. Power pattern of the uniform inspired and inspired with optimum coupling (OC) ordinary end-fire antenna arrays for (a) $d = 0.25\lambda$, (b) $d = 0.1\lambda$ inter-element spacings. Bottom halves of the figures (a) and (b) present the HPBW.

- Frequency of interest, $f = 1$ GHz.
- ULA composed of 20 identical dipole antennas.
- The undesired coupling matrices, $\boldsymbol{C}$ for a 0.5λ-wavelength antenna system with different inter-element distances ($d = 0.25\lambda$ and $d = 0.1\lambda$), are calculated according to [7, chapter 8] for finite-length thin-dipole antennas.
- The antennas are located on the z-axis parallel to the y-axis; then assuming azimuth $\phi = 90^\circ$ (on the y–z plane, see figure 2), the element factor for a finite-length dipole antenna is computed as

$$\mathrm{EF}(\theta, 90^\circ) = \left[\frac{\cos(\frac{kl}{2}\sin\theta) - \cos(\frac{kl}{2})}{\cos\theta} \right], \qquad (15)$$

where $k = \frac{2\pi}{\lambda}$, λ is the wavelength of the radiated signal and l is the length of each antenna.

Table 1. Directivity gains of the antenna arrays in the desired direction $\theta = 0^\circ$ and $\phi = 90^\circ$ (dB).

	Uniform		Binomial	
	$d = 0.25\lambda$	$d = 0.1\lambda$	$d = 0.25\lambda$	$d = 0.1\lambda$
Inspired array	19.22	16.92	16.86	15.19
Standard array	13.96	10.77	10.81	8.08

Recall that we focus on a 2D beampattern design in terms of elevation angle, θ.

We demonstrate our results for standard and inspired arrays in figures 7 and 8, and summarize the calculated directivity gains and HPBW values in tables 1 and 2, respectively. We observe that the biologically coupled inspired array with uniform excitation voltages outperforms the uniform standard array in terms of sidelobe suppression,

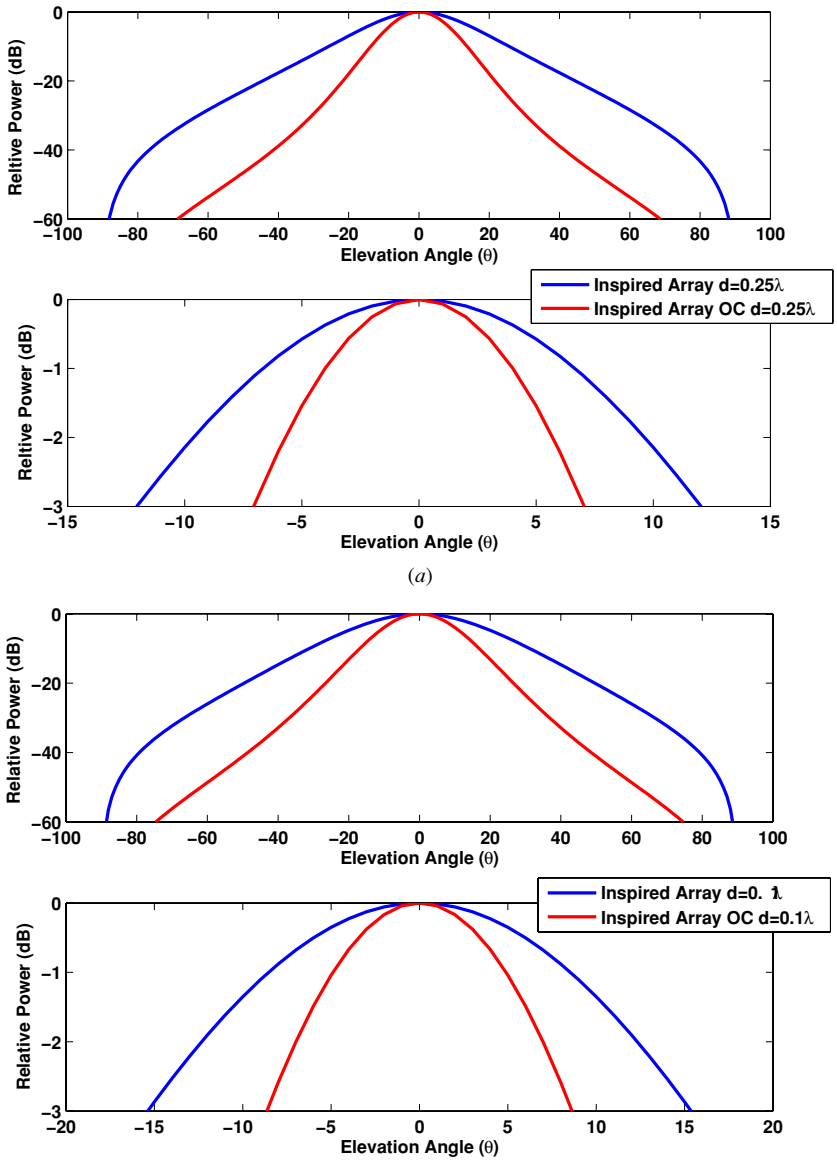

Figure 10. Power pattern of the binomial inspired and inspired with OC end-fire antenna arrays for (a) $d = 0.25\lambda$, (b) $d = 0.1\lambda$ inter-element spacings. Bottom halves of the figures (a) and (b) present the HPBW.

directivity and HPBW (see figure 7, and tables 1 and 2). For binomial array, in figure 8, we observe that neither the standard nor the inspired array have sidelobes, but the inspired array has much narrower HPBW and hence better directivity gain (see also tables 1 and 2). The physical reason of the improvement in the radiation performance is the BIC that works as a multi-input multi-output filter, magnifying the amplitude and phase differences (time differences) between the outputs of the successive antennas and creating a virtual array with a larger aperture. In the beampattern design, the virtual array with larger aperture creates a radiation pattern with higher directivity and sidelobe supression, and lower HPBW. Note that in these examples the effect of the BIC increases as the distance between the antennas, d, decreases.

In figures 7 and 8, for inspired array, we choose the coupling (the real parts of the poles of the characteristic function) manually to obtain better radiation performance than the standard antenna array. We then select the coupling parameters optimally following the algorithm described in section 4. In figures 9 and 10, we present the results on the comparison of the radiation patterns corresponding to the manually (inspired coupling used in figures 7 and 8) and optimally chosen coupling parameters. In these figures the inspired array optimum coupling (OC) corresponds to the inspired array with optimum coupling. We demonstrate that we further improve the radiation performance (both

Table 2. HPBWs of the antenna arrays (degrees).

	Uniform		Binomial	
	$d = 0.25\lambda$	$d = 0.1\lambda$	$d = 0.25\lambda$	$d = 0.1\lambda$
Inspired array	19°	28°	24°	30°
Standard array	45°	62°	63°	76°

Table 3. Directivity gains of the antenna arrays in the desired direction $\theta = 0^\circ$ and $\phi = 90^\circ$ (dB).

	Uniform		Binomial	
	$d = 0.25\lambda$	$d = 0.1\lambda$	$d = 0.25\lambda$	$d = 0.1\lambda$
Inspired array	19.22	16.92	16.86	15.19
Inspired array OC	25.62	22.16	22.75	20.35

Table 4. HPBWs of the antenna arrays (degrees).

	Uniform		Binomial	
	$d = 0.25\lambda$	$d = 0.1\lambda$	$d = 0.25\lambda$	$d = 0.1\lambda$
Inspired array	19°	28°	24°	30°
Inspired array OC	9.8°	14.6°	14.2°	17.4°

the directivity gain and HPBW) by using the optimization algorithm that we propose (see also tables 3 and 4).

6. Conclusion

We designed a coupled antenna array transmission system inspired by the mechanically coupled ears of *Ormia ochracea*. First, we obtained the response of the mechanical model representing the coupling between the *Ormia*'s ears. Then, we converted this response to the desired radio frequencies and designed the biologically inspired coupled antenna array by applying the converted response to the array factor of the antenna system. Since we focus on systems confined to small spaces, we also considered the undesired electromagnetic coupling among the array elements. We computed the radiation intensity, and accordingly the directivity gain, the half-power beamwidth and the sidelobe level of the biologically inspired and standard antenna arrays as the performance measures. We demonstrated the improvement in the radiation performance due to the biologically inspired coupling. Moreover, we showed the further improvement in the radiation performance by optimally choosing the coupling parameters. In our future work, we will focus on the implementation of the beampattern design, 3D beampattern design, design of additional biologically inspired coupling beyond the adjacent antennas, nonlinear antenna arrays (circular, etc).

Acknowledgments

Authors would like to thank Dr Carlos Muravchik of UNLP, Argentina, for his valuable comments. This work was supported by DARPA grant no HR0011-09-P-0007, the Department of Defense under Air Force Office of Scientific Research MURI grant FA9550-05-1-0443 and ONR grant N000140810849.

Appendix. Computation of the undesired electromagnetic coupling matrix C

An antenna in the transmitting mode can be modeled as in figure A1. Assuming M-element antenna array, and

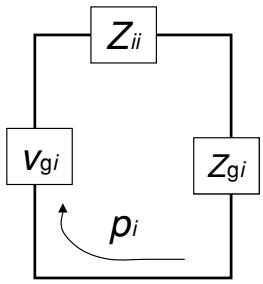

Figure A1. Circuit model of the ith antenna element in the transmitting mode.

considering the mutual effect of the other antennas in the array, the induced current on the ith antenna can be computed through (see also [7] and [21])

$$p_i(Z_{ii} + Z_g) = v_{gi} - \sum_{k \neq i}^{M} p_k Z_{ik}, \tag{A.1}$$

where,

- p_j, $j = 1, \ldots, M$, is the induced current on the jth antenna;
- Z_{jj} is the self impedance of the jth antenna;
- Z_g is the generator impedance;
- v_{gj} is the generator voltage applied to the jth antenna and
- Z_{jk} is the mutual impedance between the jth and kth antennas.

Assuming identical antennas and generators (identical self and generator impedances), we can rewrite (A.1) and obtain

$$\begin{bmatrix} Z_{11} + Z_g & Z_{12} & \cdots & Z_{1M} \\ Z_{21} & Z_{22} + Z_g & \cdots & Z_{2M} \\ & & \cdots & \\ Z_{M1} & Z_{M2} & \cdots & Z_{MM} + Z_g \end{bmatrix} \begin{bmatrix} p_1 \\ . \\ . \\ . \\ p_M \end{bmatrix} = \begin{bmatrix} v_{g1} \\ . \\ . \\ . \\ v_{gM} \end{bmatrix}. \tag{A.2}$$

Then recalling from section 2 that $\boldsymbol{p} = \boldsymbol{C}\boldsymbol{v}$, we get

$$\boldsymbol{C} = \begin{bmatrix} Z_{11} + Z_g & Z_{12} & \cdots & Z_{1M} \\ Z_{21} & Z_{22} + Z_g & \cdots & Z_{2M} \\ & & \cdots & \\ Z_{M1} & Z_{M2} & \cdots & Z_{MM} + Z_g \end{bmatrix}^{-1} \tag{A.3}$$

References

[1] Bar-Shalom Y 1987 *Tracking and Data Association* (San Diego, CA: Academic)
[2] Pavildis I, Morellas V, TsiamyrTzis P and Harp S 2001 Urban surveillance systems: from the laboratory to the commercial world *Proc. IEEE* **89** 1478–97
[3] Reddingt N J, Bootht D M and Jonest R 2005 Urban video surveillance from airborne and ground-based platforms *IEE Int. Symp. Imaging for Crime Detection and Prevention (ICDP)* (7–8 June 2005, Australia) pp 79–84

[4] Long M W 2001 *Radar Reflectivity of Land and Sea* (Dedham, MA: Artech House Publishers)
[5] Brenner A R and Roessing L 2008 Radar imaging of urban areas by means of very high-resolution SAR and interferometric SAR *IEEE Trans. Geosci. Remote Sens.* **46** 2971–82
[6] Nehorai A and Paldi E 1994 Vector-sensor array processing for electromagnetic source localization *IEEE Trans. Signal Process.* **42** 376–98
[7] Balanis C A 1982 *Antenna Theory: Analysis and Design* (New York: Wiley)
[8] Cade W 1975 Acoustically orienting parasitoids: fly phonotaxis to cricket song *Science* **190** 1312–3
[9] Robert D, Amoroso M J and Hoy R R 1992 The evolutionary convergence of hearing in a parasitoid fly and its cricket host *Science* **258** 1135–7
[10] Robert D, Read M P and Hoy R R 1994 The tympanal hearing organ of the parasitoid fly *Ormia ochracea* (Diptera, Tachinidae, Ormiini) *Cell Tissue Res.* **275** 63–78
[11] Robert D, Miles R N and Hoy R R 1996 Directional hearing by mechanical coupling in the parasitoid fly *Ormia ochracea* *J. Comp. Physiol.* A **179** 29–44
[12] Robert D, Miles R N and Hoy R R 1998 Tympanal mechanics in the parasitoid fly *Ormia ochracea*: intertympanal coupling during mechanical vibration *J. Comp. Physiol.* A **183** 443–52
[13] Mason A C, Oshinsky M L and Hoy R R 2001 Hyperacute directional hearing in a microscale auditory system *Nature* **410** 686–90
[14] Miles R N, Robert D and Hoy R R 1995 Mechanically coupled ears for directional hearing in the parasitoid fly *Ormia ochracea* *J. Acoust. Soc. Am.* **98** 3059–70
[15] Akcakaya M and Nehorai A 2008 Performance analysis of *Ormia ochracea*'s coupled ears *J. Acoust. Soc. Am.* **124** 2100–5
[16] Kay S M 1993 *Fundamentals of Statistical Signal Processing: Estimation Theory* (Upper Saddle River, NJ: Prentice Hall)
[17] Tucker D G 1967 Superdirective arrays: the use of decoupling between elements to ease design and increase bandwidth *Radio Electron. Eng.* **34** 251–6
[18] Newman E, Richmond J and Walter C 1978 Superdirective receiving arrays *IEEE Trans. Antennas Propag.* **26** 629–35
[19] Popovic B D, Notaros B M and Popovic Z 1999 Supergain antennas: a novel philosophy of synthesis and design *Proc. 26th URSI General Assembly (Toronto, Ontorio, Canada)* p 7675
[20] Lee T and Wang Y E 2008 Mode based information channels in closely coupled dipole pairs *IEEE Trans. Antennas Propag.* **56** 3804–11
[21] Allen J L and Diamond B L 1966 *Mutual Coupling in Array Antennas* (*Technical Report* 424) (Lexington, MA: MIT Lincoln Laboratory)
[22] Gupta I and Ksienski A 1983 Effect of mutual coupling on the performance of adaptive arrays *IEEE Trans. Antennas Propag.* **31** 785–91
[23] Svantesson T 1998 The effects of mutual coupling using a linear array of thin dipoles of finite length *Proc. 9th IEEE SP Workshop on Statistical Signal and Array Processing* pp 232–5
[24] Akcakaya M, Muravchik C H and Nehorai A 2010 Biologically inspired antenna array and direction of arrival estimation *Proc. 44th Asilomar Conf. Signals, Systems and Computers (Pacific Grove, CA, 7–10 November)*